# Hydraulic fracturing technology for improving permeability in gas-bearing coal seams in underground coal mines

by B.X. Huang[*], C.M. Huang[†‡], Q.Y. Cheng[‡], C.H. Huang[§], and W.C. Xue[*]


## Synopsis

Hydraulic fracturing technology is presented as a solution to improve permeability and thus solve the extraction problem of coal seam gas in low-permeability gas-bearing coal seams. Given an existing group of original cracks, the propagation of main hydraulic cracks and hydraulic wing cracks was simulated using realistic failure process analysis software. The process represents the structural transformation of hydraulic fracturing and permeability improvements caused by it. In addition, a field test for improving the permeability of gassy coal seams by hydraulic fracturing was also conducted. The propagation of the main cracks and wing cracks by hydraulic fracturing forms a network of original joint cracks, hydraulic wing cracks, and main hydraulic cracks, which improve the permeability of the coal seam. High-pressure water in the drill hole and in the main hydraulic cracks permeates the two flanks of the hole, forming the permeating water pressure. With an increase in drill water pressure and an extension of the main hydraulic cracks, the permeating water pressure on both sides of the main hydraulic cracks in the coal mass also increases. Hydraulic cracks tend to form connections through rock bridges. The extension of hydraulic wing cracks through connections in the rock bridges between the cracks transforms the rock mass to a fractured structure and improves its permeability. Hydraulic fracturing technology for improving permeability in underground conditions can increase the amount of gas drainage by a factor of 15. A stress relief area develops at a radial distance of 10–20 m from the hydraulic fracturing drill hole, while an area of rising stresses, called the pressurized area, develops a further 15 m away from the pressurized hole. Practice has proved the existence of the stress transfer phenomenon and the high stress area after fracturing. This kind of hydraulic fracturing technology is more effective in holes drilled from underground than in surface drill holes, with respect to costs and controllability, and is therefore the major trend in gas drainage development in coal mines.



**Keywords**

coal seam, gas, hydraulic fracturing, crack propagation, improving permeability.


## Introduction

China has a total of 825 high-gas coal mines (state-owned coal mines and state-owned local mines). Most of these coal seams have low permeability, and some even have a high adsorption capacity and poor desorption, such as the Xishan Mine Area. There are 274 pairs of coal and gas outburst mines around the country, representing 45 per cent of the total number of the world's outburst mines. China has the highest prevalence of coal and gas outburst accidents in the world, with more than 11 500 recorded accidents, leading to the most serious mining death toll in the world.

Hydraulic fracturing technology applications in the oil industry are very mature. Much research has been directed toward the flow, stress, and damage (FSD) coupling damage behaviour of hydraulic fracturing[1–3], filtration law[4], filtration and the impact of pore pressure gradient formed by filtration on the hydraulic crack tip cracking[5–6], crack tip stress perturbations[7], repeated fracturing[8], and geophysical monitoring of hydraulic fracturing[9]. Currently, hydraulic fracturing technology has been applied to many other industries. The techniques used in natural gas extraction through drilling of surface wells have been applied to the extraction of coal-bed gas by hydraulic fracturing technology[10–12], but there are still many problems to study.

A coal mine is different from an oil field. The underground tunnels connect directly with the coal seam, so providing a space for underground hydraulic fracturing operations. Based on this, techniques for improving the permeability of gas-bearing coal seams in underground coal mines by hydraulic fracturing have beendeveloped. The underground drills for improving the permeability of the coal seam (thereby weakening it) for hydraulic fracturing are


* *School of Mines, China University of Mining and Technology, Xuzhou, China.*

† *The first Shoushan coal mine of Pingbao Coal Mining Corporation, Xuchang, China.*

‡ *Faculty of Safety Engineering, China University of Mining and Technology, Xuzhou, China.*

§ *The tenth mine of Pingdingshan Coal Mining Corporation, Pingdingshan, China.*


 *Paper received Jan. 2012; revised paper received Feb. 2012.*

arranged around the mining area. The drill holes are mostly horizontal or inclined. During mining, the stress field distribution around the drill is very complex and dynamic[13]. Because the oil drill and coal seam gas drills are directed mostly from the surface, the rock surrounding the fracturing drill is basically in the original state of stress, and the stress distribution remains relatively stable. A coal mass is a brittle medium in which joint cracks develop well[14], and the integrity of rock fractured from surface wells is significantly better than that of coal seams. Because of the physical and mechanical properties of the coal mass and the impact of mining, the methods and technology of weakening a coal mass and improving its permeability by hydraulic fracturing cannot replicate those used in the oil industry. Hydraulic fracturing practices employed in coal mines have already proven this point.

## Technology of hydraulic fracturing for improving permeability

In hydraulic fracturing of coal seams, the borehole water pressure is used to change the stress state in the coal mass adjacent to the borehole, leading to crack initiation and propagation (Figure 1). Fissure water pressure is used to control the extension of the main hydraulic crack. Meanwhile, with the expansion of the main hydraulic crack, water under pressure penetrates into both sides of the cracks. The infiltration water pressure can cause further extension of the original cracks, which extend generally perpendicular to the direction of minimum principal stress, resulting in a certain angle between the expanded wing crack and the original crack surface. The increased crack density in the coal rock mass can improve the connectivity of the crack network. Adding proppant (fine sand) increases the size of the crack openings, and the network formed by the original joint cracks, wing cracks, and the main hydraulic cracks can improve the coal seam permeability. Meanwhile, crack extension not only leads to structural damage but also weakens the overall coal mass. Moreover, sufficient moisture and absorption further weaken the coal seam itself[15]. The key is to control the hydraulic crack initiation and extension and to have a good knowledge of the relationship between the spatial distribution of structural changes and permeability changes in the coal mass under water pressure.

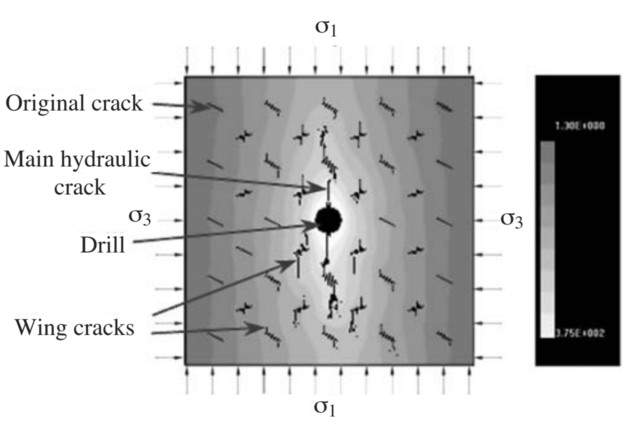


**Figure 1—Hydraulic pressure distribution in the rock surrounding a hydraulic fracturing drill**

## Structural changes in the coal rock mass induced by hydraulic fracturing

A large amount of research in coal mines has shown that the original cracks in the coal seam often occur in groups. Within the horizontal projection plane, they form a pair of parallel cracks or two staggered parallel cracks. Fissure water pressure resulting from water penetration will cause extension of the original crack wing, leading to destruction of the coal microstructure. In order to demonstrate some possible mechanisms of fracture network formation, simple two-dimensional numerical simulation models of hydraulic fracturing were established by using realistic failure process analysis (RFPA) software. The morphology and structural damage caused by the main hydraulic crack and wing crack extension and the effects of different numbers of original crack groups on hydraulic crack extension were simulated and analysed.

### *A brief introduction to RFPA*

RFPA was developed by Professor Tang Chunan of the Dalian University of Technology. It is a variety of numerical test software that can simulate the progressive failure of a material[2,16]. The calculation method is based on finite-element theory and statistical damage theory. This method takes into account the nonuniformity of material properties and the random distribution of defects. In the RFPA system, after the stress solver completes the stress and strain calculation for each element, the program is transferred to a phase-change analysis mode, which checks each element's phase change based on phase transformation criteria. According to the type of phase change, the phase-change elements are processed by weakening stiffness (such as cracks or separation) or rebuilding stiffness (such as compaction or exposure). Finally, the elements' new physical and mechanical parameters for the whole medium, which are used for the iterative calculation, are generated. The material's microdefects can be simulated by a special mapping tool that considers the joints, cracks, and other macroscopic defects. The RFPA$^{2D}$ system has the function of simulating and analysing the phenomena of flow–structure interaction (such as hydraulic fracturing, water inrush, or rock seepage), gas–solid coupling (coal and gas outbursts), and temperature–stress field coupling[2].

### *Numerical simulation program*

A cubic coal specimen with a section of 500 × 500 mm was taken as the test model. A two-dimensional model was established for the specimen section. Using the plane strain method, the specimen was divided into 200 × 200 units. The numerical simulation program is shown in Table I and Figure 2. The modified Mohr-Coulomb strength criterion, which takes the tension rupture of the rock material into account, is accepted as the failure criterion of rock[2]. In the test, the drilling water pressure was increased stepwise to simulate the hydraulic fracturing process. In Program 1, an equably distributed group of cracks of 90 mm spacing, void ratio of 0.2, length of 25 mm, and angle of 15° was used. Program 2 adds a group of cracks with the same crack density and angle as the previous program. A hole 50 mm in diameter is then drilled into the centre of the block. The water pressure on the drill wall is increased in steps of 0.25 MPa from an initial pressure value of 0 MPa.

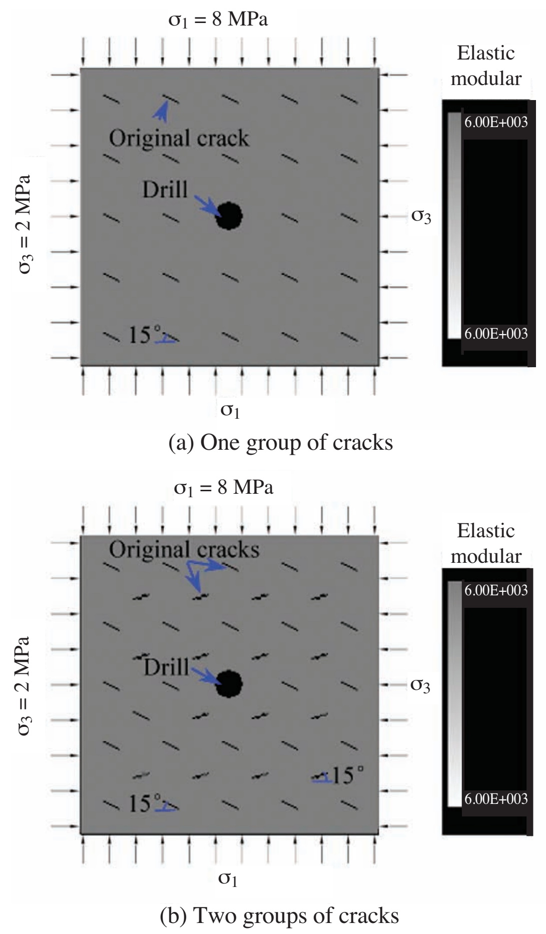


**Figure 2—Numerical simulation models**

*Table I*

**Numerical simulation program**

| Parameter | Value | Parameter | Value |
|---|---|---|---|
| Modulus of elasticity (*E*) | 6000 MPa | Degree of uniformity | 1000 |
| Compressive strength ($\sigma_c$) | 20 MPa | Degree of uniformity | 100 |
| Fissure inclination | 15° | Pore water pressure coefficients | 0.5 |
| Horizontal loading pressure | 2 MPa | Vertical loading pressure | 8 MPa |
| Internal friction angle | 32° | Circular hole diameter | 50 mm |
| Initial water pressure | 0 MPa | Water pressure increment per step | 0.25 MPa |

In the simulation, the flow, stress, and damage coupling model is accepted as the solid–liquid coupling model[2]. This model takes into account not only the gradual expansion process of the hydraulic crack tip, but also the water seepage at the crack tip, stress, and damage coupling. The viscosity of water is 1.0050 × $10^{-3}$ Pa·s. The effect of water seepage as a function of time can also be reflected through a set-up of iterative times and time span for dynamic problems under the given water pressure in the seepage time option. The output results are the shear stress, acoustic emission, the elastic modulus, and a hydraulic contour map.

## *Analysis of simulation results*

### *Expansion law for the main hydraulic crack*

The structural damage morphology of hydraulic fracturing under the conditions of just one group of original cracks is shown in Figure 3. Pressure water within the borehole penetrates the surrounding rock, increasing the pore water pressure. In the nonhydrostatic stress field, the pore water pressure contour formed by penetration has an oval-shaped distribution: the maximum hydraulic gradient is in the direction of minimum principal stress ($\sigma_3$), while the minimum hydraulic gradient is in the direction of maximum principal stress ($\sigma_1$). With increasing distance from the drill, the hydraulic gradient decreases.

Under the coupling action of the pore water pressure and the *in situ* stress, in the model with a single set of 15° angle cracks, the orifice began to crack when the water pressure reached 1.25 MPa, whereas the main hydraulic crack extended stably when the water pressure was in the range of 3–3.25 MPa. Hydraulic cracks expanded perpendicularly to the minimum principal stress direction. The crack tip was most likely to initiate tension rupture along the direction of the minimum hydraulic gradient, leading to hydraulic crack propagation. Therefore, it can be said that under the action of *in situ* stress, hydraulic cracks extend along the direction of the minimum pore water pressure gradient. When the water pressure was 3.5 MPa, the main hydraulic crack was close to the original cracks. Because the rock bridges (i.e. areas of unfractured rock spanning the distance between two crack

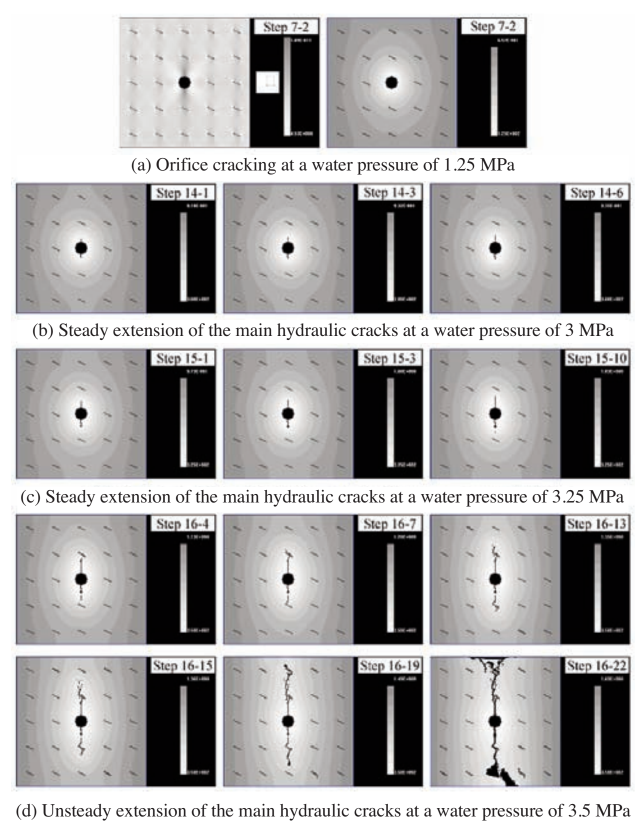


**Figure 3—Macro–micro structure damage from the hydraulic fracture model of one group of original cracks**

tips) between the main hydraulic crack tips and the original cracks were short, the extension direction of the main hydraulic crack was deflected. The main hydraulic crack and the original wing crack expanded through the lower part of the model but not in the upper part of the model, though they had a similar trend; the main hydraulic crack continued extending along the other side of the original wing cracks.

### *Expansion law for the wing crack*

High-pressure water penetrated around the drilling hole and the two sides of the main hydraulic crack, increasing the hydraulic seepage pressure. With the increase of drilling water pressure and the extension of the main hydraulic crack, the seepage pressure in the rock mass on both sides of the main hydraulic crack also increased. In the model with one group of original cracks, under the *in situ* stress field, the original cracks produced wing cracks gradually, but, overall, their length was relatively short.

Double groups of original cracks had an impact on the crustal stress. The existence of original cracks leads to stress concentration near the crack tips (Figure 4). Groups of cracks propagating together intensified the local stress concentration in the rock, and microcracks appeared in the right-trending group (Figure 5a). Under the impact of drilling pressure relief, orifice cracking occurred when the drill water pressure was 0 MPa. Around the drill, the further extension of the original cracks formed microcracks, followed by wing cracks.

With time and an increase in drilling water pressure, the pore water pressure in the surrounding rock increases. The coupling between pore water pressure and skeletal stress led to an increase in the stress intensity factor of the main hydraulic crack and wing crack tips. At a drill water pressure of 3 MPa, the main hydraulic crack extended steadily, and the original wing cracks also expanded along the direction perpendicular to the direction of minimum principal stress. At a water pressure of 3.75 MPa, the main hydraulic crack extended intermittently, and it connected with the original wing crack through the rock bridge (Figure 5c). The main hydraulic crack continued to extend along the other end of the wing crack. With the increase of permeating water pressure, the length of the hydraulic wing cracks grew (Figure 6). Because the pore water pressure on both sides of the model was relatively smaller, the extension of the original cracks was significantly smaller than that near the main hydraulic cracks.

### *Effect of hydraulic fracturing on coal permeability and gas desorption*

Gas exists mainly within the pores of the coal seam. For efficient extraction of gas, we must enhance coal porosity, fracture (cleat) and the connectivity to drilling, ease of gas desorption, seepage, and diffusion. The extension of the main hydraulic crack and wing crack played a role in increasing the cutting degree to coal seam, thus resulting in a structural transformation of the fractured coal mass. The main hydraulic crack and wing cracks increased the fracture density within the coal seam and improved the gas flow channels between the pores and the drill hole, thereby increasing the permeability of the coal seam.

Under the influence of high-pressure water, the stress state of the coal mass changes due to internal displacement, and structural damage ensues. The extension of hydraulic

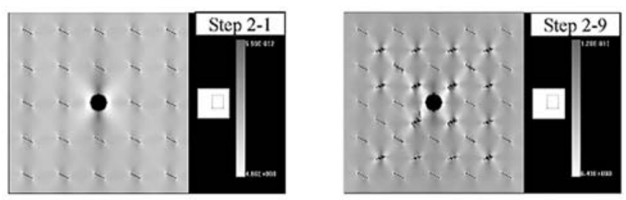


(a) One group of original cracks (b) Two groups of original cracks

**Figure 4—Shearing stress distribution at a water pressure of 0 MPa**

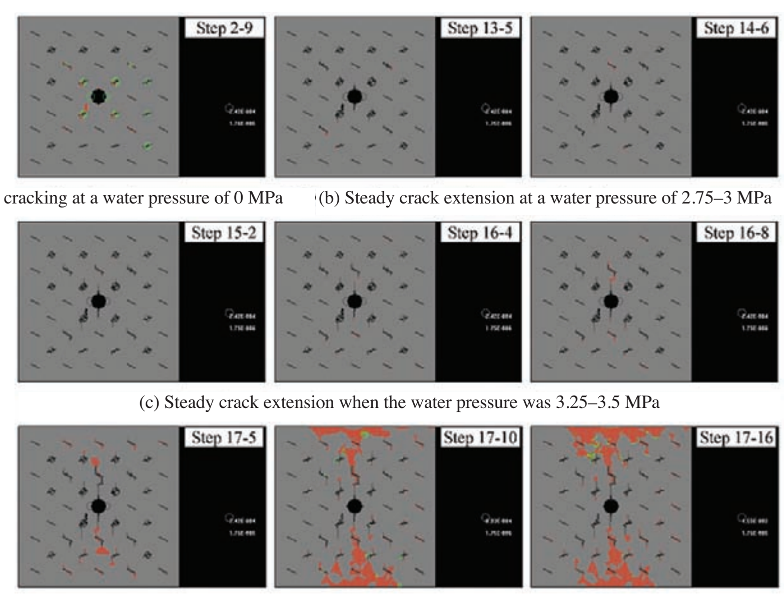


(a) Orifice cracking at a water pressure of 0 MPa (b) Steady crack extension at a water pressure of 2.75–3 MPa

(c) Steady crack extension when the water pressure was 3.25–3.5 MPa

(d) Intermittent crack extension at a water pressure of 3.75 MPa

**Figure 5– Acoustic emission from the hydraulic fracture model of two groups of original cracks**

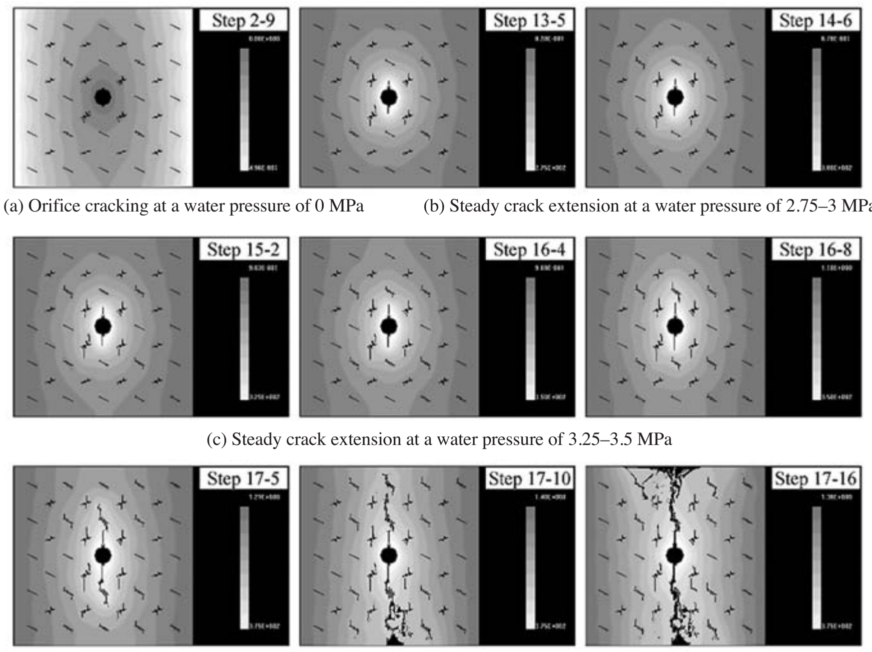


(a) Orifice cracking at a water pressure of 0 MPa (b) Steady crack extension at a water pressure of 2.75–3 MPa

(c) Steady crack extension at a water pressure of 3.25–3.5 MPa

(d) Intermittent crack extension at a water pressure of 3.75 MPa

**Figure 6—Hydraulic pressure distribution from the hydraulic fracture model of two groups of original cracks**

cracks reduces the stress in some parts, which improves gas desorption owing to pressure relief. Meanwhile, after the water permeates the coal mass, the physical effect of water on the coal and gas is very complex. Water in the coal mass significantly inhibits gas emission, and can reduce the desorption rate of adsorbed gas. Therefore, coal-bed methane extraction by hydraulic fracturing should be undertaken using a high flow rate of water to induce rapid fracturing, increase the pressure range of crack extension, and reduce the infiltration of fracturing fluid, which will be conducive to subsequent gas drainage.

## Test programme for hydraulic fracturing to improve permeability in underground coal mines

### *General situation at the working face*

The tenth mine of the Pingdingshan Coal Mining Corporation is located in the eastern part of Pingdingshan, and was put into operation in February 1964. The mine's gas emissions have increased every year. In 2008, the absolute emission of gas was 130.20 $m^3$/min, and the relative emission was 33.48 $m^3$/t, which was the largest emission from any Henan coal mine.

The test site was the haulage tunnel of the $F_{15}$-24080 working face, F-4 district of the tenth coal mine of Pingdingshan. The ground elevation is +150 to +280 m, and the working face elevation is –580 to –660 m. The average inclined length of the working face is 188 m, and the strike length is 1804 m; the thickness of the $F_{15}$ coal seam is between 1.6 and 2.3 m (generally around 2 m). The structure of the coal seam is simple. Its dip angle is relatively gentle in the eastern part of the district, usually about 10°. In the middle and upper parts, the dip angle is larger, being about 25°–30°, whereas it is usually about 20° in the western part.

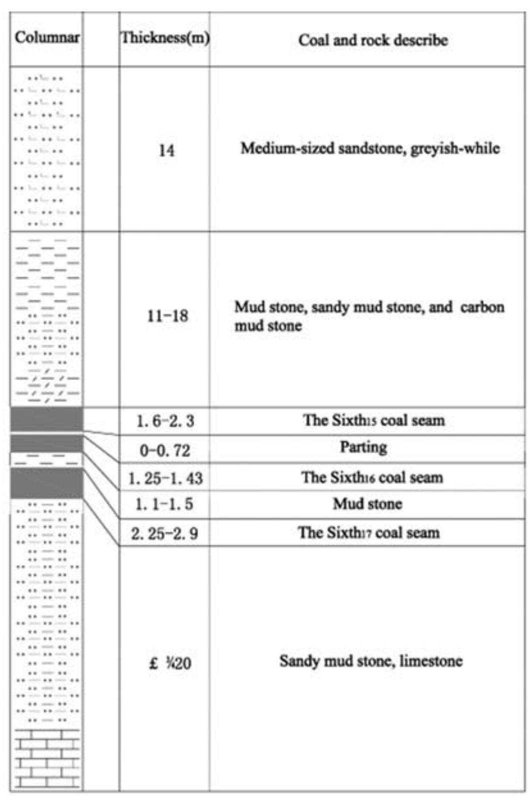


**Figure 7—Stratigraphy of the $F_{15}$-24080 working face**

The coal seam roof of the $F_{15}$-24080 working face is mudstone and sandy mudstone, with a thickness of 11–18 m. The $F_{16}$ coal seam, which is 1.25–1.43 m in thickness, is beneath the $F_{15}$ coal seam, and its floor strata is shale of 1.1–1.5 m thickness (Figure 7). A parting layer of 0–0.72 m separates the two coal seams. The $F_{15}$ coal seam has a hardness coefficient of 0.24–0.37, and the original moisture content of the coal mass is 0.94 per cent. The coal seam of the working face has a gas pressure of 2.4 MPa and a gas content of 30 $m^3/t$, which makes it an outburst seam. The seam has a poor permeability coefficient of only 0.0013 mD (Millidarcy), which makes extracting gas from the coal seam sometimes difficult.

## Implementation plan

### *Equipment*

The following equipment is used:

- *Fracturing pump*—type BRW400/31.5 emulsion pump for the coal mine, with a rated pressure of 31.5 MPa and a rated flow of 400 L/min.
  Water tanks: iron, with a volume of 3 $m^3$.
  Pressure gauge: type YHY60 (B) digital pressure gauge of intrinsic safety type for coal mines.
  Handheld collector: type FCH32/0.2 intrinsic safety type for coal mines.
- *Pipeline*—High-pressure pipeline: selected high-pressure hoses with inner diameters of 25 and 38 mm and corresponding compressive strengths of 38 and 35 MPa.
  Seamless steel tube: external diameter of 38 mm, inner diameter of 27 mm, and pipe thickness of 5.5 mm, with the length of each section being 3 m. The inner tube wall of the drill packer was open with a drill density of 10 holes per metre, and the bottom of the steel tube was closed.
- *Drill packer*—special capsule drill packer, with compressive strength of not less than 35 MPa, external diameter of 55 mm, length of 5–20 m and pressure expansion coefficient of 40 per cent.
- *Drilling tool*—Drilling rig: the first type of production drill hole used a type CMS1-1200/30J hydraulic deep drill rig for coal mines, produced in Jiangyin. Its drill pipe was a spiral with $\Phi$ = 100 mm, and bit of $\Phi$ = 120 mm. These rigs were used for the drilling construction before and after fracturing; the second type used a type ZL-1200 electric coal drill, produced in Chongqing. Its drill pile was of $\Phi$ = 50 mm, and its bit of $\Phi$ = 66 mm. These rigs were used for the fracturing drilling.
- *Electromagnetic radiation instrument*—type KBD5 electromagnetic radiation instrument of intrinsic safety type for coal mines for coal and gas outbursts.
- *Injection pump*—type 2ZBQ-11.5/3, with a rated pressure of 3 MPa and a rated flow of 11.5 L/min.

### *Process*

The process is as follows: Water supply pipe → Water tank → Connecting pipe → Water injection pump → High-pressure water pipe → Special drill packer → Drill a hole → Coal mass.

### *Implementation*

A total of seven coal seam hydraulic fracturing tests were conducted. The F15-24080 haulage tunnel coal seam, the test holes, and observation holes had already been arranged when the two hydraulic fracturing tests were conducted (Figure 8). In addition, the water pressure curve of hydraulic fracturing, observational data, and other test results were also completed beforehand.

#### *Specifications for hydraulic fracturing hole drilling and sealing*

- *No. 1 fracturing drill hole*—The specifications of the No. 1 hole are as follows: depth = 50 m, elevation = 15°, diameter = 66 mm, and distance from the No. 2 fracturing hole = 68 m. A special capsule sealing device was used, with a length of 20 m and a sealing depth of 25 m. The observation hole was sealed with cement mortar. Within the fracturing area, the drainage hole was sealed with polyurethane. The drainage hole was connected with an 8-inch drainage pipe for gas extraction.
- *No. 2 fracturing drilling hole*—The specifications of the No. 2 hole were identical to those for hole No. 1.

#### *Process of hydraulic fracturing*

To obtain the coal seam fracturing pressure and other parameters, a smaller displacement was adopted in the No. 1 hydraulic fracturing hole, and the measured displacement during the test was 120–140 L/min. The water pressure for hydraulic fracturing is shown in Figure 9. First, a pressure regulation test was conducted. After water injection for 3 minutes the water pressure reached 12 MPa, and the hole wall began to rupture. The rupture water pressure of the coal seam was therefore considered to be 12 MPa. After the initiation of rupture, the water pressure dropped sharply to 7 MPa for 6 minutes. Pumping was then stopped for 6 minutes, and the water pressure slowly dropped because of infiltration of the coal seams. After 13 minutes of additional pumping, formal fracturing began. By 16 minutes the water pressure rose to 14 MPa and repeated water pressure fluctuations occurred, but the overall water pressure trend was upward, indicating that within the coal seam several small hydraulic cracks had opened in the expansion. By 21 minutes

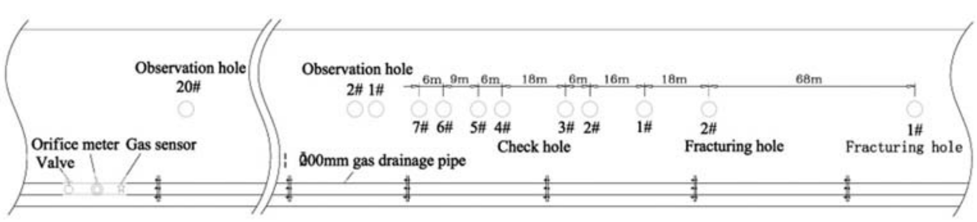


**Figure 8—Layout of the hydraulic fracturing holes in the haulage tunnel**

the water pressure had risen to 15 MPa, after which there was a substantial decline, indicating a larger hydraulic crack expansion. Fluctuations in water pressure occurred, and then the pressure continued to rise until reaching a maximum value of 16 MPa. Then, overall, the water pressure trended downward and essentially stabilized after 73 minutes at a value of 14.4–14.6 MPa. Crack extensions caused the water pressure to drop to 12 MPa or so, further corroborating our finding that the fracturing pressure of the coal seam was 12 MPa. At 216 minutes, the pump was turned off. At 221 minutes, the water was drained to relieve water pressure, and conditions near the hole were observed. At 321 min, pumping resumed and the water pressure quickly rose to 14 MPa. Because the closed crack, which had been fractured, opened up again, the fracturing pressure dropped sharply to 11 MPa. Water pressure then gradually increased to 15.8 MPa, and then dropped drastically to a steady 14.5 MPa. At 380 minutes after the first rapid decrease of water pressure, the pressure dropped to 8.2 MPa and remained unchanged. The unchanged pressure value indicated that given the pump displacement, the hydraulic fracture had extended to the tunnel or other free space and would not continue extending. The pump was turned off to stop fracturing at 391 minutes. At 398 minutes, the water was drained to relieve pressure. The total fracturing time was 279 minutes and 35 $m^3$ of fracturing fluid had been pumped.

Field observations of the No. 1 hole fracturing test showed that there was considerable water running from the predrainage holes and bolt holes of the haulage tunnel and some water running linearly at some bolt trays. The most distant water was draining as far as 36 m from the fracturing hole, indicating that the extent of fracturing had reached 36 m. The joint and crack of the coal seam were relatively well developed, so the infiltration was large. The hydraulic fracturing pressure of 120–140 L/min displacement fluctuated significantly, indicating that the pump displacement was not adequate. Insufficient displacement resulted in fracturing of long duration, too low a water pressure, and limited crack propagation. Therefore, hydraulic fracturing of underground coal seams should use a high-flow high-pressure fracturing pump.

The measured pump displacement of the No. 2 hole was about 200 L/min. When the water pressure reached 15 MPa, it stabilized for 5 minutes, and the drill hole wall ruptured, forming hydraulic cracks. In this condition, therefore, the coal seam fracturing pressure was 15 MPa. Field tests proved that increasing the displacement of the coal seam pump will lead to an increase in the fracturing pressure. The water pressure quickly increased after the infusion of water, stabilizing at 26–28 MPa at 16 minutes. After 80 minutes of pumping, the water pressure rapidly decreased to 24 MPa, followed quickly by a rise to 28 MPa. At 83 minutes, the pump was stopped to make observations for safety reasons, so the water pressure quickly dropped to 0 MPa. Pumping was continued after 13 minutes of observation, and the water pressure stabilized at 26 MPa. At 137 minutes, the water pressure began to fluctuate rapidly between 22–28 MPa for 18 minutes. This showed that the hydraulic cracks may extend to a huge surface structure. Pumping was stopped at 155 minutes. The total fracturing time was 2 hours and 36 minutes and 21 $m^3$ of fracturing fluid of had been pumped.

During the hydraulic fracturing test of the No. 2 hole, water flowed from the scrapped drainage hole 76.4 m away from the fracturing hole. That was because a fault zone (with a gap of 1 m) connected the scrapped drainage hole with the fracturing cracks. The fault was located about 53 m away from the final fracturing hole. This shows that the maximum radius of the fracturing zone was 53 m or more. On the whole, the water pressure curve of the No. 2 hole was much smoother than that of the no. 1 hole. The water pressure and the fracturing crack propagation range of the No. 2 hole were significantly greater than those of the No. 1 hole, but the No. 2 hole used only 60 per cent of the amount of water in the No. 1 hole. Coal seam hydraulic fracturing technology therefore needs to adopt a high-flow pump and a fast fracturing technology to increase the fracture extension range and reduce the fracturing fluid infiltration, which would be conducive to subsequent gas drainage. During the hydraulic fracturing test, no water permeated out from the fracturing hole, indicating that the use of a special sealing device could meet the hydraulic fracturing sealing requirements in a coal seam dipping at 13°.

## Test analysis

### *Effect of gas drainage*

Single-hole gas drainage volume before and after hydraulic fracturing

For the No. 1 hole, the nearest drainage hole to the fracturing hole, before fracturing, the largest single-hole gas density was 14 per cent, the largest gas drainage flow rate was 0.0087 $m^3$/min, the cumulative drainage flow rate for

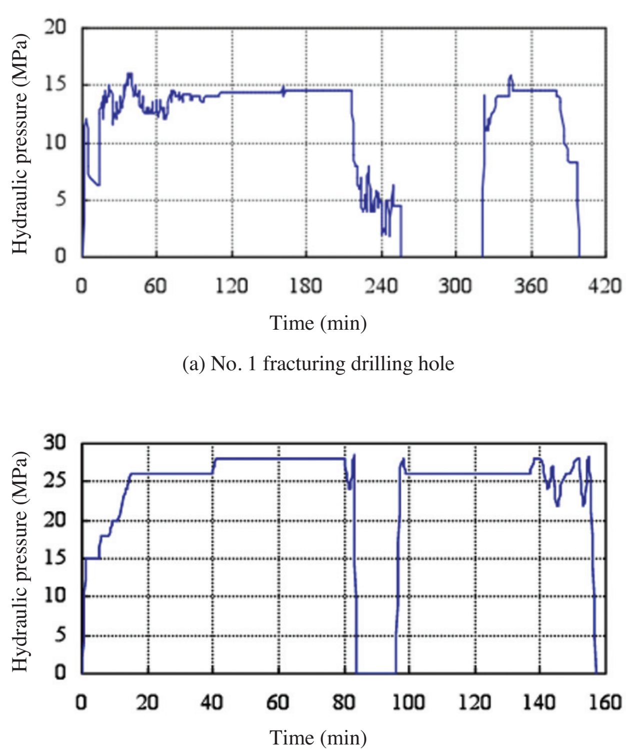


**Figure 9—Water pressure curve for hydraulic fracturing**

20 days was 0.0354 m³/min, and the attenuation period was about 7 days (Figure 10). After fracturing, the largest single-hole gas density was 26 per cent, the largest gas drainage flow rate was 0.0144 m³/min and the cumulative gas drainage flow rate for 20 days was 0.2018 m³/min (Figure 11). After fracturing, the single-hole gas drainage volume had increased by a factor of 5.9 over that before fracturing in the same period, and the attenuation period had been prolonged significantly.

### *Two-group hole gas drainage volume before and after fracturing*

Each group consisted of seven holes. Before fracturing, the largest single-hole gas density was 20 per cent, the largest gas drainage flow rate was 0.0130 m³/min, the cumulative drainage flow rate for 20 days was 0.1380 m³/min and the average gas drainage flow rate was 0.0011 m³/min (Figure 12). After fracturing, the largest single-hole gas density was 26 per cent, the largest gas drainage flow rate was 0.0144 m³/min, the cumulative gas drainage flow rate was 2.0737 m³/min, and the average gas drainage flow rate was 0.0148 m³/min. After fracturing, the gas drainage volume had increased by a factor of 15 over that before fracturing.

### *The change of gas pressure before and after fracturing*

The original coal seam gas pressure before fracturing was 2.4 MPa. Within the radius of influence of the fracturing, the measured residual gas pressure was 0.02 MPa after drilling and drawing the gas out.

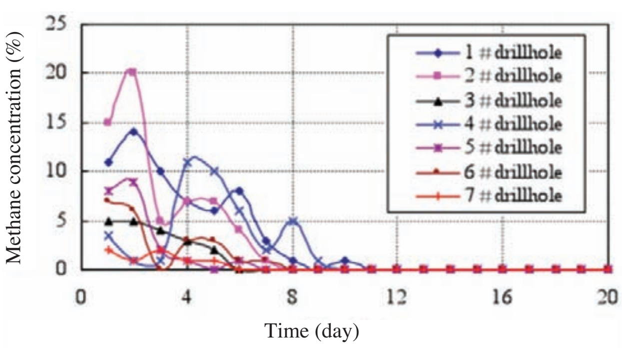


(a) Gas density

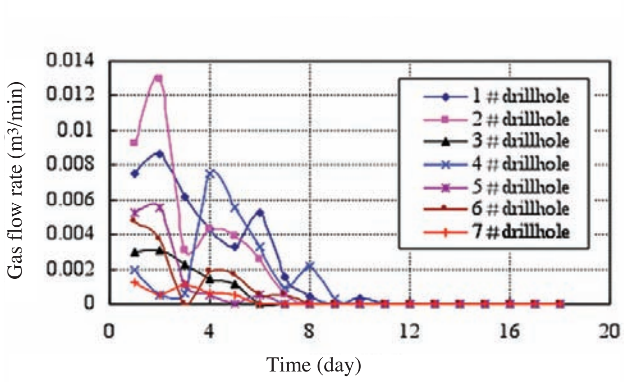


(b) Gas drainage flow rate

**Figure 10—Drilling hole gas drainage volume changes before fracturing**

### *Fractured radius and changes in moisture*

Before fracturing, by testing the drilling sample, the original moisture content of the coal mass was 0.94 per cent. After hydraulic fracturing, a hole was drilled every 10 m from the fracturing hole and samples at hole depths of 20 and 40 m were analysed for moisture content. The results are shown in Figure 13.

According to the test results, the moisture content of the coal mass was between 1.2 per cent and 2.89 per cent; the moisture content 60 m away from the hydraulic fracturing hole was 1.2 per cent, close to the original moisture content of 0.94 per cent. According to the raw data, the water injection moist radius under static pressure was 3–5 m. It can be therefore be determined that the fracturing radius under 29 MPa pressure is 55–57 m.

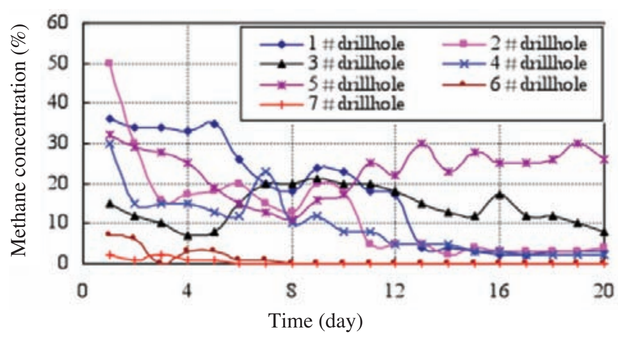


(a) Gas density

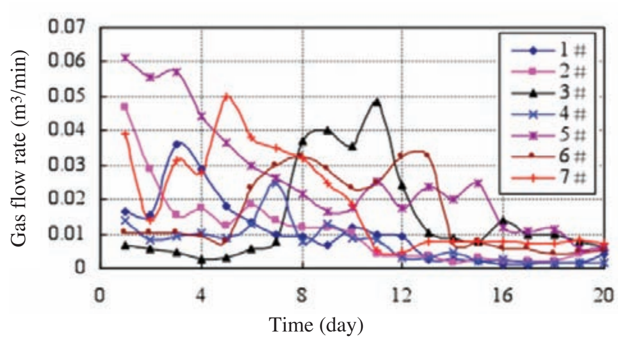


(b) Gas drainage flow rate

**Figure 11—Drilling hole gas drainage volume changes after fracturing**

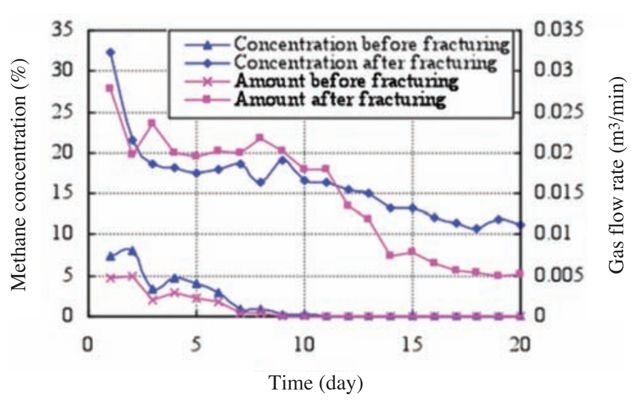


**Figure 12—Comparison of the average drill gas drainage effect before and after fracturing**

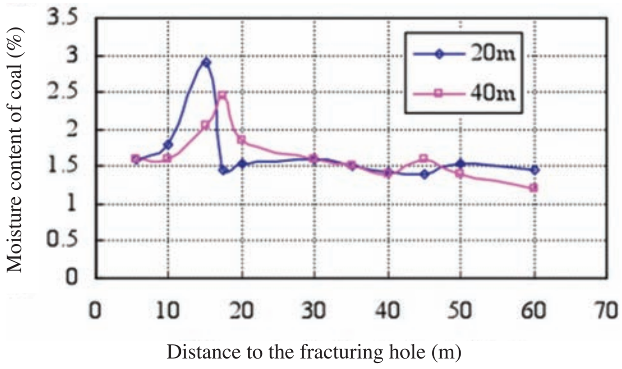


**Figure 13—Changes in moisture content with distance from fracturing hole**

### *Stress variation before and after fracturing near the fracturing drilling hole*

During the two hours before and after the fracturing test, a KDB5 electromagnetic radiation (ER) instrument was used to measure the electromagnetic radiation intensity for a distance of 120 m on each side of the fracturing hole. The results are shown in Figure 14.

The average ER intensity was 27 mV before fracturing and 35 mV after fracturing, an increase of 8 mV (30 per cent). The average intensity value around the fracturing hole dropped from 30 mV before fracturing to 20 mV. The general electromagnetic radiation intensity and pulse count after fracturing had increased compared with the values before fracturing. The largest increase in average intensity was 11 mV overall. Within 25 m of the fracturing hole, the increase in intensity was lower, with the largest increase being 9 mV. At distances greater than 25 m, the intensity increase was much more significant, and the largest average intensity increase was 14 mV. This demonstrates that the gas content and stress distribution of the coal mass around the fracturing hole had moved. Within 10–20 m on two sides of the centre of the hydraulic fracturing drill hole, a stress relief area developed; a further 15 m outside, there developed an area of increased stress (pressurized area).

Problems with a jetting hole and a sticking tool were encountered when drilling was conducted to a depth of 10–20 m before fracturing. However, after fracturing, few abnormal phenomena were observed within 30 m of the hydraulic fracturing hole at a depth of 45–75 m. This shows that the original rock stress and gas stress of the coal mass had been transferred to the deeper part after fracturing, causing the abnormalities to move to greater depth. As the distance between the drilling and the fracturing hole increased, the depth at which the drilling abnormalities emerge began to decrease gradually. The drilling crumbsweight, the intensity and duration of jetting, and other abnormal phenomena were more pronounced than in the area beyond 30 m of the fracturing hole. This indicates that the gas near the hydraulic fracturing hole is transferred to the two sides of the hole, which verifies the existence of the stress transfer phenomenon and the high stress area after fracturing.

From the ER measurement results, after hydraulic fracturing the pulse counts and pulse amplitude in the coal mass within 10 m around the hydraulic fracturing hole both decreased significantly, leading to a decrease in the peak value of abutment pressure and a shift in peak positions to the deeper part of the coal wall. Thus hydraulic fracturing plays a role in controlling coal and gas outbursts.

## Comparative analysis of the improved permeability resulting from hydraulic fracturing through a surface well

### *Social benefits*

- The gas drainage density of the coal mass after hydraulic fracturing is greatly increased. Full use of high-density gas (so far used mainly for power, about 7000 kWh per day) has reduced atmospheric pollution caused by gas emissions, achieving the aims of energy savings, emission reduction, and environmental protection
- After hydraulic fracturing, gas drainage reduces the gas content and gas pressure in the coal mass and the internal stress distribution of the coal mass is altered, thus reducing the chance of coal and gas outbursts or pressure bumps and ensuring safer production
- After hydraulic fracturing, the increase of the moisture content in the coal mass is reduced, as is the amount of dust created during mining, thus improving the working environment
- The equipment for hydraulic fracturing technology is simple and easy to operate, and requires only a small investment.

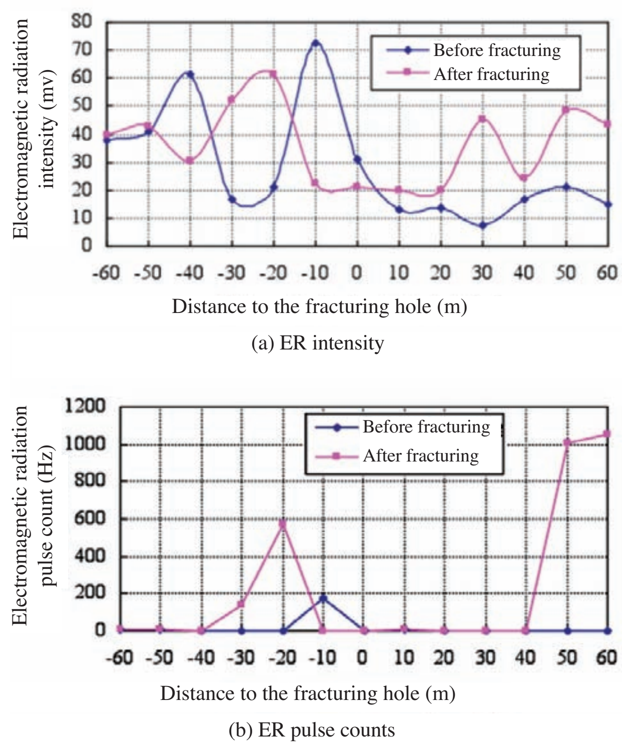


**Figure 14—ER curves before and after fracturing**

### Economic benefits

Cost estimates for hydraulic fracturing through a surface drilling well are shown in Table II. The reasonable range of applicability for hydraulic fracturing technology through surface drilling is an ellipsoid with a major axis radius of 100 m and a minor axis radius of 30 m, with a total area of 9420 m$^2$. The total cost of hydraulic fracturing is 2.162 million yuan RMB (6.3 yuan ≈ 1 US dollar), and the cost per unit area is about 229.5 yuan.

Cost estimates for hydraulic fracturing in an underground tunnel are shown in Table III. So far, the influence range of hydraulic fracturing in an underground mine is about 50 m long and 40 m wide, for an area of 2000 m$^2$. The total cost is 55500 yuan, or about 27.75 yuan per unit area.

This comparison between surface and underground hydraulic fracturing shows that underground drilling can save considerable costs (201.75 yuan per unit area, representing an 88 per cent reduction) compared with surface drilling.

### Comparison with surface hydraulic fracturing technology

#### Gas drainage rate and controllability

The drilling depth for surface hydraulic fracturing is greater, making the projects larger. In addition, surface hydraulic fracturing requires a lot of casing to ensure coal seam fracturing. This results in a certain risk of layer location control in fracturing. China's current success rate for gas drainage of coal-bed methane wells is about 40 per cent. Conducting hydraulic fracturing in underground coal mines is easier to accomplish than from surface. The drilling depth is relatively less, and the drilling direction is easy to control. After fracturing, the drilling hole can serve as a gas drainage hole as well, but drilling a specialized gas drainage hole around the fracturing hole in a mine is also feasible. The success rate of drilling gas drainage from underground is 100 per cent.

#### Impact on mine water inrush

For surface coal-bed gas wells, the coal seam is mined during their service period. During mining, wells can easily act as channels for mine water inrush if there is water in the overlying strata. Underground coal seam drilling hydraulic fracturing technology needs only short drilling depths, and the length of hydraulic fracture extension is relatively short. Underground drilling therefore has no impact on mine water inrush.

#### Impact on strata control of the surrounding rock

Both surface and underground hydraulic fracturing

*Table II*

**Hydraulic fracturing cost for a surface well**

| No. | Item | Unit price (yuan/m) | Subtotal (10 000 yuan) | Remarks |
|---|---|---|---|---|
| 1 | Space expense | | 6 | |
| 2 | Moving expense | | 15 | Drilling, fracturing, etc. |
| 3 | Drilling cost | 900 | 56 | Calculated for 800 m |
| 4 | Casing pipe cost | 400 | 36 | Including surface casing and technical casing |
| 5 | Mud logging cost | 150 | 12 | Calculated for 800 m |
| 6 | Well cementation cost | | 20 | |
| 7 | Well logging cost | 140 | 11.2 | Calculated for 800 m |
| 8 | Coring cost | 5000 | 3 | Calculated for 6 m thick coal seam |
| 9 | Well testing expense | | 15 | |
| 10 | Mud pit and drilling water costs | | 2 | |
| 11 | Hydraulic fracturing cost | | 40 | |
| | Total | | 216.2 | |

*Table III*

**Hydraulic fracturing costs for an underground drill hole**

| No. | Item | Unit price (yuan/m) | Subtotal (10 000 yuan) | Remarks |
|---|---|---|---|---|
| 1 | Moving expense | | 1.0 | |
| 2 | Drilling cost | 50 | 0.25 | |
| 3 | Hole sealing cost | 5000 | 0.5 | Based on 50 m |
| 4 | Fracturing cost | | 3.0 | |
| 5 | Test cost | | 0.3 | |
| | Drilling water cost | | 0.5 | |
| | Total | | 5.55 | |

technology for improving permeability and weakening the coal seam influence how effectively the surrounding rock can be controlled. Relatively speaking, with underground hydraulic fracturing it is easier to control the fracture morphology extension than with surface hydraulic fracturing. Underground hydraulic fracturing therefore has a relatively smaller impact on the strata control of surrounding rock.

### *Impact on coal and gas outbursts*

Because of the objective existence of the stress transferring phenomenon and the high stress area after hydraulic fracturing, no final conclusion regarding the effect of hydraulic fracturing on coal and gas outburst risk can be reached. If hydraulic fracturing causes a local stress concentration, it may increase the risk of coal and gas outbursts. Because underground hydraulic fracturing makes it easier to control the morphology of hydraulic fracturing cracks than surface hydraulic fracturing, an underground fracturing programme can be optimized through the interaction of adjacent fracturing to minimize the impact of local stress concentrations caused by single-hole hydraulic fracturing on coal and gas outbursts.

### *Summary*

Given the aspects of costs, controllability, the success rate of gas drainage, the impact on mine water inrush, the impact on coal and gas outbursts and risk control, underground hydraulic fracturing technology is superior to hydraulic fracturing technology using wells drilled from surface. Thus, a major trend has developed towards underground drilling hydraulic fracturing technology for gas drainage in coal mining.

## Conclusions

- The extension of the main hydraulic crack and wing cracks during hydraulic fracturing forms a network consisting of the original joint cracks, hydraulic wing cracks, and the main hydraulic crack, which improves the permeability of the coal seam
- High-pressure water in the drill and in the main hydraulic crack permeates the two flanks, forming the permeating water pressure. With increasing drill water pressure and extension of the main hydraulic crack, the permeating water pressure on both sides of the main hydraulic crack in the coal mass also increases
- Hydraulic cracks tend to connect through rock bridge lines. The extension of hydraulic wing cracks and the connections of rock bridges among the cracks lead to a transformation of the fractured rock structure and improve the permeability of the rock mass
- Technology for improving permeability using hydraulic fracturing in underground conditions has greatly improved drill gas drainage. After hydraulic fracturing, the gas drainage volume can be increased by a factor of 15 over that before fracturing
- Within 10–20 m on two sides from the centre of the hydraulic fracturing drill hole, a stress relief area is created; 15 m further out, an area of increased stress (pressurized area) forms. Experience has proved the existence of the stress transfer phenomenon and the high stress area after fracturing.
- Coal seam hydraulic fracturing technology needs to adopt high-flow pumps and fast fracturing technology to increase the fracture extension range and reduce the infiltration of fracturing fluid, which is conducive to subsequent gas drainage
- Improved permeability technology using hydraulic fracturing in underground coal mines is superior to surface-well fracturing in terms of controllability and economics. Thus there is a major trend towards the use of underground drilling for gas drainage in coal mining.

## Acknowledgements

Financial support for this work, provided by the National Natural Science Foundation of China (No. 51004104) and the National Basic Research Program of China (No. 2011CB201200), is gratefully acknowledged.

## References

1. Ruiting, W. Some fundamental mechanisms of hydraulic fracturing. PhD. thesis, *Georgia Institute of Technology*, Georgia, 2006. p. 16.
2. Tang, C.A., Tham, L.G., and Lee, P.K.K. Coupling analysis of flow stress and damage (FSD) in rock failure. *International Journal of Rock Mechanics and Mining Sciences*, vol. 39, no. 4, 2002. pp. 477–489.
3. Papanastasiou, P.C. A coupled elastoplastic hydraulic fracturing model. *International Journal of Rock Mechanics and Mining Sciences*, vol. 34, no. 3–4. 1997 pp. 240–254.
4. Piggott, A.R. Static and dynamic calculation of formation fluid displacement induced by hydraulic fracturing. *Applied Mathematical Modelling*, vol. 20, 1996. pp. 714–718.
5. Lenoach, B. The crack tip solution for hydraulic fracturing in a permeable solid. *Journal of the Mechanics and Physics of Solids*, vol. 43, no. 7, 1995. pp. 1025–1043.
6. Ito, T. Effect of pore pressure gradient on fracture initiation in fluid saturated porous media: Rock. *Engineering Fracture Mechanics*, vol. 75, 2008. pp. 1753–1762.
7. Rahman, M.K and Joarder, A.H. Investigating production-induced stress change at fracture tips: Implications for a novel hydraulic fracturing technique. *Journal of Petroleum Science and Engineering*, vol. 51, 2006. pp. 185–196.
8. Zhang, G.Q. and Chen, M. Dynamic fracture propagation in hydraulic re-fracturing. *Journal of Petroleum Science and Engineering*, vol. 70, 2010. pp. 266–272.
9. Ishida, T. Acoustic emission monitoring of hydraulic fracturing in laboratory and field. *Construction and Building Materials*, vol. 15, 2001. pp. 283–295.
10. Warren, T.M. and Hayatdavoudi, A. Hydraulic fracturing thin coal seams in preparation for *in situ* gasification. *Mechanical Engineering*, vol. 99, no. 2, 1977. pp. 139–139.
11. Zuber, M.D., Reeves S.R., Jones, A.H., and Schraufnagel, R.A. Variability in coal bed methane well performance—A case study. *Journal of Petroleum Technology*, vol. 43, no. 4, 1991. pp. 468–475.
12. Olovyanny, A.G. Mathematical modeling of hydraulic fracturing in coal seams. *Journal of Mining Science*, vol. 41, no. 1, 2005. pp. 61–67.
13. Huang, B.X. Research on theory and application of hydraulic fracture weakening for coal-rock mass. PhD thesis, China University of Mining and Technology, 2009.
14. Chertkov, V.Y. and Ravina, I. Networks originating from the multiple cracking of different scales in rocks and swelling soils. *International Journal of Fracture*, vol. 128, no. 1–4, 2004. pp. 263–270.
15. Huang, B.X., *et al.* Hydraulic fracturing theory of coal-rock mass and its technical framework. *Journal of Mining Safety and Engineering*, vol. 28, no. 2, 2011. pp. 167–173.
16. Tang, C. and Zhao, W. RFPA2D system for rock failure process analysis. *Chinese Journal of Rock Mechanics and Engineering*, vol. 16, no. 5, 1997. pp. 507–508. ◆